Electronic Supplementary Material (ESI) for Journal of Materials Chemistry C.

This journal is © The Royal Society of Chemistry 2019

Supporting Information

Laser Fabricated Nanometer-thick Carbon Film and Its Strain-Engineering for Achieving Ultrahigh Piezoresistive Sensitivity

*Jiangjiang Luo, Xiaoshuang Duan, Zhepeng Chen, Xiaojun Ruan, Yanbo Yao and Tao Liu**

College of Chemistry, Chemical Engineering and Materials Science, Soochow University, Soochow, No. 199 Renai Road, Soochow City, 215123, P.R. China

E-mail: tliu@suda.edu.cn

Experimental Section

Preparation of ultrathin carbon film on a fused silica substrate by DLWc and its transfer to a polyimide substrate: A vacuum spin coater (VTC-200P, Shenyang Branch Crystal Automation Equipment Co., Ltd.) was used for preparing polyamic acid (PAA) thin film on a fused silica with size of 50 mm × 50 mm × 1 mm (SiO_2 ≥99.98%, Lianyungang Xinben Fused quartz Co., Ltd) at room temperature and relative humidity < 50%. Before spinning coating operation, the stock solution of PAA (YE1001, 20 wt. % solid content, Shanghai Wild Wo Industry and Trade Co. Ltd.) was diluted to 1 - 7wt. % by molecular sieve dried N, N-dimethylformamide

(DMF, ≥ 99.8%, Aladdin - full name) for controlling the film thickness. The fused silica was also surface treated/cleaned by O_2 plasma (ZEPTO, Shanghai Erdi Instrument Technology Co., Ltd.) for 1 minute prior to spin coating. The same spinning condition was applied to prepare all PAA film samples in our study, which included three sequential steps: step 1 – constant spinning speed at 1000 rpm for 30 sec; step 2 – constant spinning speed at 2000 rpm for 30 sec; and step 3 – constant spinning speed at 5000 rpm for 30 sec. Subsequent to spin coating process, the wet PAA films was heat treated at 100 ^oC for 1h,150 ^oC for 1.5 h and 300 ^oC for 1 h following this order to give polyimide (PI) thin film ready for direct laser writing carbonization (DLWc) process. A laser engraving and cutting machine equipped with a CO_2 laser of wavelength 10.6 μm (SCE4030, Wuhan Sunic Photoelectricity Equipment Manufacture Co., Ltd.) was used to apply DLWc operation on the PI film prepared above. In the DLWc process, a line scanning laser writing mode was adopted with laser power, laser scanning speed and line-to-line interval respectively set at 1.5 W, 10 mm/s and 50 μm to fabricate the square-shaped ultrathin carbon film with size of 3 mm × 3 mm. To transfer the as-formed ultrathin carbon film on the fused silica to a polymer substrate, e.g., polyimide (PI), we adopted a solution cast and film peeling off process. In brief, a thin layer of PAA solution (20 wt. %) was spun cast onto the fused silica, on which the ultrathin carbon film was formed, by using a two-step spinning condition: step 1 – constant spinning speed at 1000 rpm for 30 sec; and step 2 – constant spinning speed at 2000 rpm for 30 sec. Following the spin coating process, the same heat treatment protocol as described above was applied

to convert PAA into a PI film, which was then peeled off readily with the ultrathin carbon film intimately adhered.

Electrical and piezoresistive property measurement and strain-engineering of the ultrathin carbon film for enhancing its piezoresistive sensitivity: The I−V behavior and the sheet resistance of the ultrathin carbon films being transferred onto a PI film was measured at room temperature by a Keithley 3706A system switch/multimeter and a Keithley 2182A nanovoltmeter with current injection applied by a Keithley 6221 current source. For selected film samples, we also tested their temperature-dependent electrical property with temperature controlled by a liquid nitrogen cooling accessory system of Q800 dynamic mechanical analyzer (DMA, TA instruments). During such test, the temperature was ramped from -100 to +100 ^{o}C at a rate of 5 ^{o}C /min. By following the procedure disclosed in our previous work,[1-3] we performed coupled electrical−mechanical test by using the Q800 dynamic mechanical analyzer to evaluate the piezoresistive behavior of the ultrathin carbon film on a PI substrate at 35 °C. The sample used for this test had a dimension of 25 mm × 6 mm. During the test, a tensile deformation was applied through force-control mode. The typical testing protocol was to ramp the force at a rate of 1 N/min to achieve the final strain up to 2 %. In the meantime, the electrical resistance of the ultrathin carbon film was measured by a Keithley 3706A system switch/multimeter equipped with a 3721 dual 1 × 20 multiplexer card at a sampling rate of 1/s. To enhance the piezoresistive sensitivity of the ultrathin carbon films, we also designed a strain engineering procedure to intentionally introduce micro/nano cracks in the ultrathin carbon film.

During the strain engineering process, the ultrathin carbon film on a PI substrate of size 25 mm × 6 mm was stretched at a constant force rate 1N/min while its resistance was monitored. The crack formation was signified by an abrupt rise of the resistance at a certain critical strain level. When this sudden resistance increase occurred, the film sample was further stretched to allow the resistance value to reach above 100 MΩ to complete the strain engineering process.

Morphology and structure characterization of the ultrathin carbon films with or without nano cracks: The morphology of the as-prepared, transferred and strain engineered- ultrathin carbon films were examined by optical microscopy (OM, MP41, Guangzhou Mingmei Optoelectronic Technology Co., Ltd.), scanning electron microscope (SEM, Hitachi SU8010), and atomic force microscopy (AFM, Bruker Dimension Icon). Transmission electron microscopy (Hitachi HT7700 and Tecnai F20) were also performed to observe the order/disorder graphitic structure of the ultrathin carbon films. The TEM sample was prepared by gently scraped off the as-prepared carbon film from the fused silica substrate with a doctor blade and then dispersed in ethanol by sonication. The suspension was then dropped onto a 325-mesh copper grid and dried at room temperature for TEM observation. The chemical structures of the ultrathin carbon films were characterized by attenuated total reflection infrared spectroscopy (Nicolet IS50), backscattering Raman scattering spectroscopy (LabRam HR800 confocal Raman microscopy, 50 × objective, 514 nm excitation wavelength) and X-ray photoelectron spectroscopy (XPS, ESCALAB 250

XI). The optical and electronic property of the ultrathin carbon film was measured by using UV-Vis-NIR optical absorption spectroscopy (200 – 2000 nm).

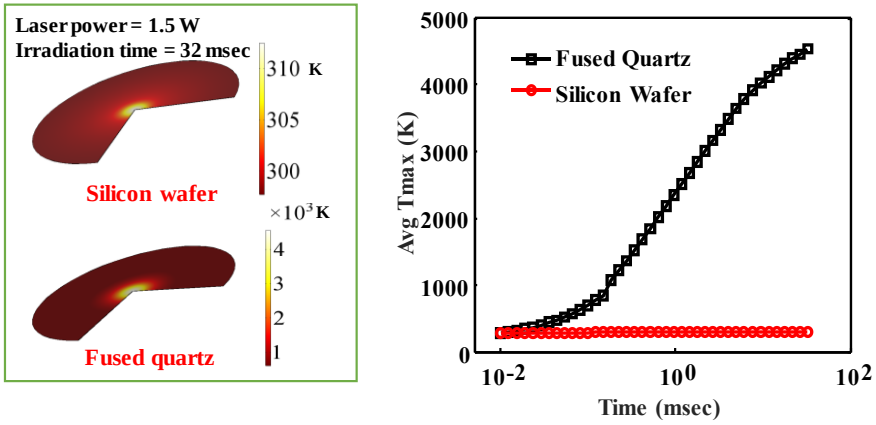

Fig S1. Photothermal modeling and simulation results on temperature rise of a thin PI film (1 μm) on a fused quartz and a silicon wafer under 1.5 W CO_2 laser irradiation for varied time duration.

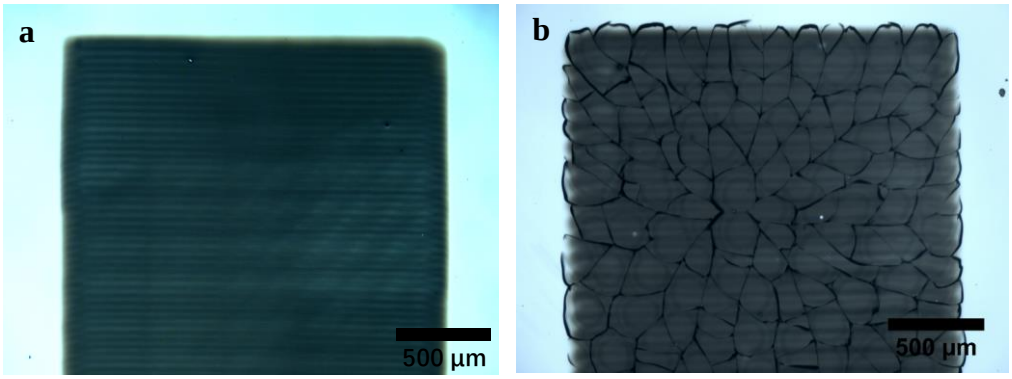

Fig S2. Optical images of the ultrathin carbon films fabricated by DLWc on a fused quartz (a) and a microscope glass slide (b). Both films were fabricated with laser power = 1.5 W and at a beam scanning speed = 10 mm/sec.

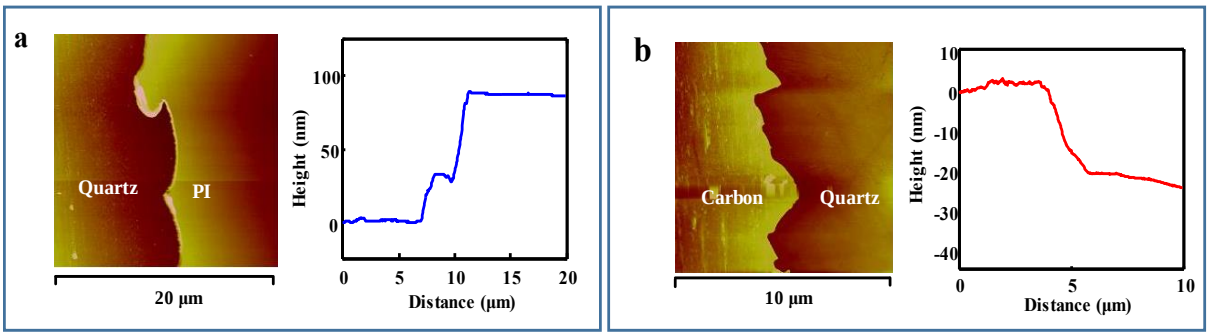

Fig S3. AFM height image of a representative PI thin film (a) and ultrathin carbon film (b) prepared from 3wt. % PAA on quartz substrate.

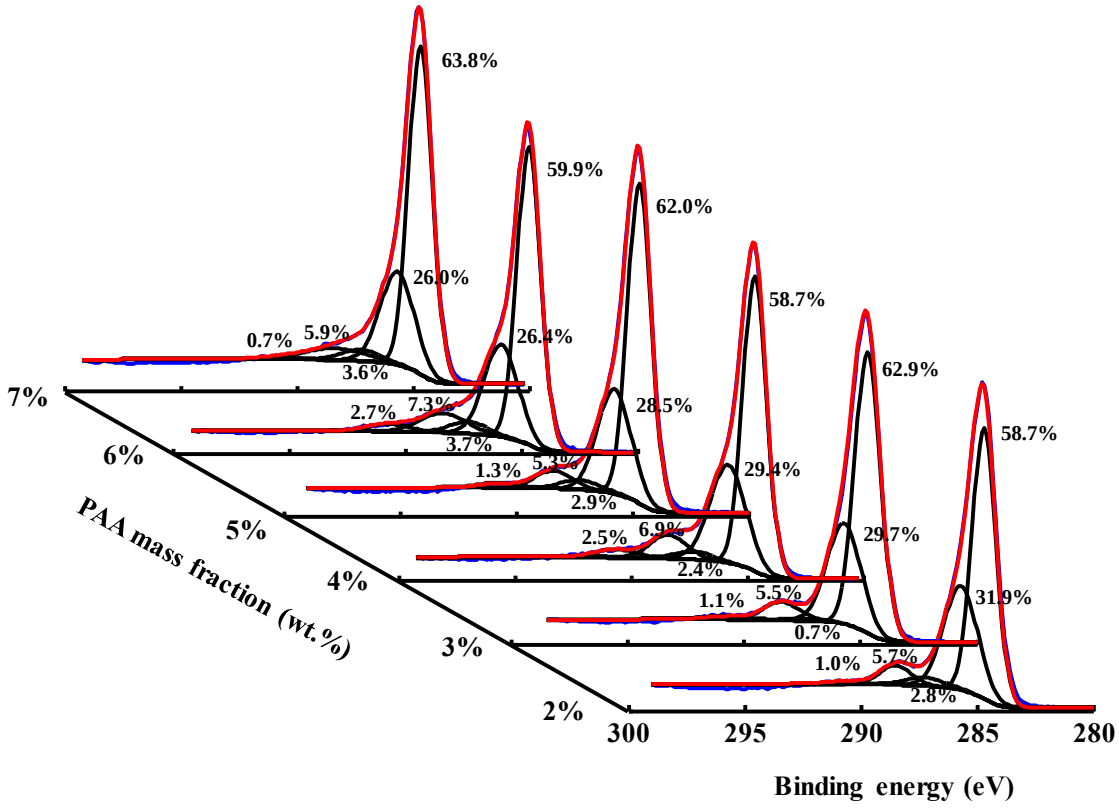

Fig S4. Peak-resolved high-resolution XPS C_{1s} spectra for the ultrathin carbon film samples prepared from 2%-7% wt. PAA solution. The resolved five peaks include graphitic sp2 carbon at 284.7 eV, carbon with phenolic, alcohol, or C=N functional groups (285.5 -285.7 eV), carbonyl or quinone groups (287.4 -287.7 eV), carboxyl or ester groups (288.0-288.6 eV) and satellite peak due to π–π* transition in an aromatic system (289.6-290.0 eV).

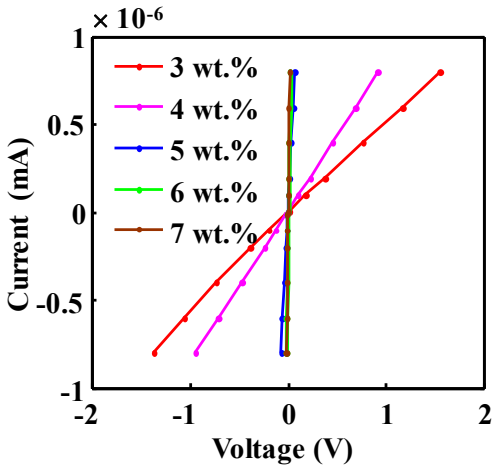

Fig S5. I-V behavior of the ultrathin carbon films prepared from 3 - 7 wt. % PAA solution.

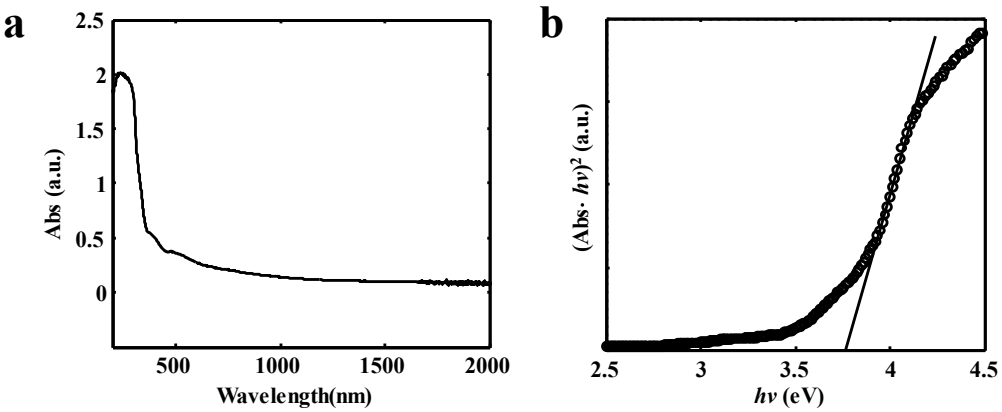

Fig S6. (a) UV–Vis absorbance spectrum of an ultrathin carbon film prepared from 7 wt. % PAA solution; (b) Tauc plot of the result shown in (a) for estimating the band-gap energy of the ultrathin carbon film, which is about 3.75 eV.

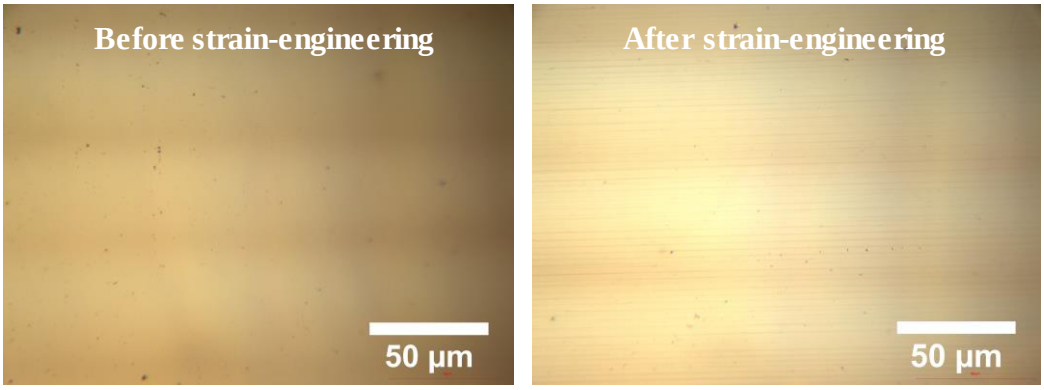

Fig S7. Optical micrographs of the ultrathin carbon film prepared from 5 wt. % PAA solution before (left) and after (right) strain-engineering treatment. The straight-line features appeared in the strain-engineering sample but free from the pristine sample extend across the entire width of the sample.

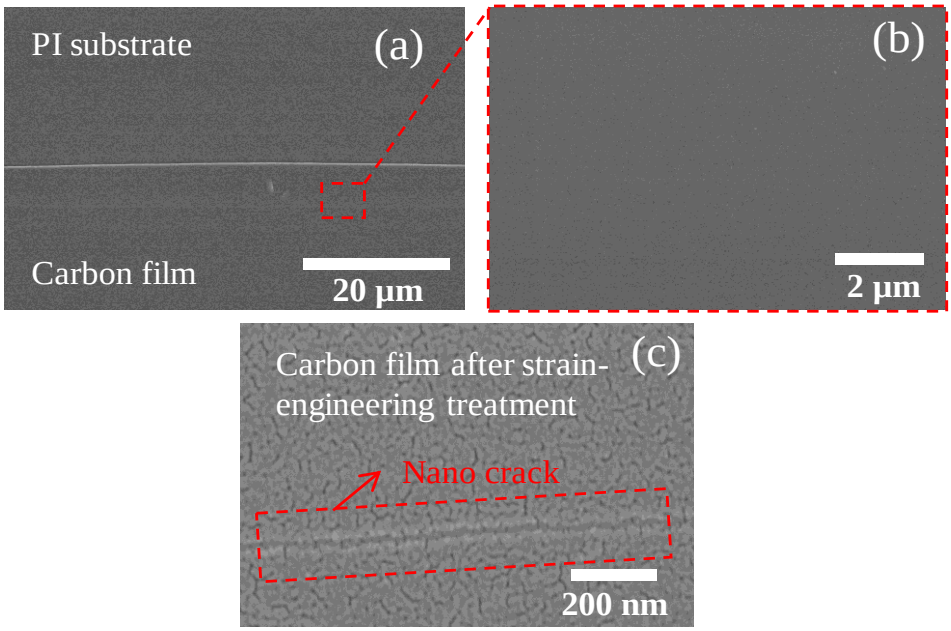

Fig S8. SEM imaging to reveal (a, b) the smooth surface morphology of the as-prepared ultrathin carbon film being transferred to a PI substrate; (c) Nanocrack formation upon strain-engineering treatment. The short and curved crack features in (c) are due to artifacts introduced by gold coating in SEM sample preparation.

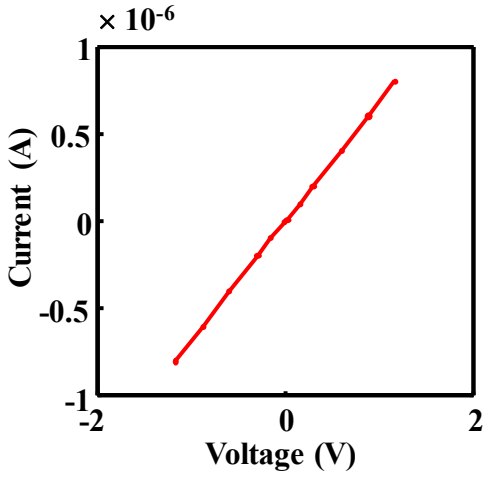

Fig S9. I-V behavior of an ultrathin carbon film with thickness of 52 nm prepared from 4 wt. % PAA after strain-engineering treatment.

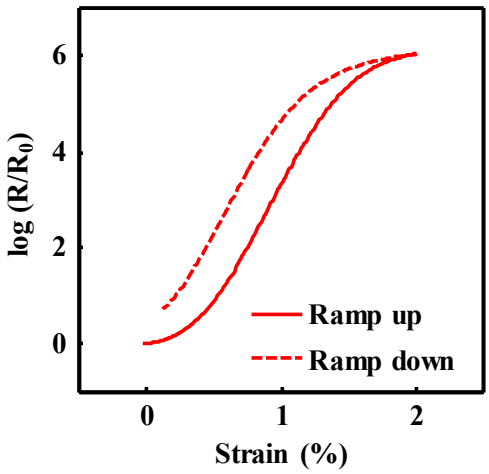

Fig S10. Hysteresis of the piezoresistive behavior of the strain-engineered ultrathin carbon film with thickness of 52 nm prepared from 4 wt. % PAA solution.

Table S1. Summary of the strain-to-failure and GF results for all ultrathin carbon film samples being studied in this work

PAA Conc. (wt. %)	Sample ID	Film Thickness (nm)	Before Strain-Engineering Treatment			After Strain-Engineering Treatment	
			Strain-to-failure (%)	Gauge Factor	Strain for GF evaluation (%)	Gauge Factor	Strain for GF evaluation (%)

7	1	180	1.85	1.46	0 < ε < 1.84	322,931	1.32
	2		2.51	2.42	0 < ε < 2.49	3,142	1.16
	3		3.13	2.66	0 < ε < 1.67	454,832	1.46
	4		1.90	1.17	0 < ε < 1.86	154,752	1.84
	5		2.33	1.07	0 < ε < 2.32	39,293	1.92
	6		2.84	1.28	0 < ε < 2.82	74,268	1.74
	7		Not Tested			10,135	1.04
	8					86,547	1.88
6	1	94	1.94	1.50	0 < ε < 1.93	129,535	1.33
	2		1.85	1.36	0 < ε < 1.83	63,741	2.86
	3		Not Tested			296,034	2.14
	4					479,358	1.81
	5					3,124	1.16
5	1	59	1.46	1.45	0 < ε < 1.45	2,271	3.45
	2		1.99	1.65	0 < ε < 1.98	49,773	1.50
4	1	52	1.74	1.23	0 < ε < 1.72	21,150	2.00
	2		2.35	1.72	0 < ε < 2.33	204	1.05
3	1	22	2.88	1.63	0 < ε < 2.86	45	0.94

Table S2. Summary of gauge factor (GF) and the corresponding strains used for GF evaluation at small deformation (strain <5%) repored in the literature

Active Sensing Element	Substrate	Fabrication Method	Gauge factor	Strain for GF evaluation (%)	Durability (Strain/Cycles)	Ref./ Published year
Strain – engineered ultrathin carbon film	PI	Direct laser writing	100-30000	0 <ε< 1%	1% / >1000	This work/2019
			30000-470000	1% <ε< 2%		
SiC	Elastomer	Direct laser writing	854	0 < ε < 3.5%	4% /10000	[4]/2018
			122060	3.5 %< ε < 5%		
Cracked Pt	PUA/PET	Depositing	2282	ε=2%	2%/1000000	[5]/2018
Au nanoparticles	PDMS	Sputter-coating	945	0 < ε < 1.5%	±0.7%/50	[6]/2018
			5888	1.5%< ε < 2%		
Au nanoparticles	PDMS film and fiber	Evaporation	<2	ε<5%	50% / 5000	[7]/2018

MWCNT/RGO@PU sponge	PU sponge	Dip-coating	<1	$0 < \varepsilon < 5\%$	Not tested	[8]/2018
SWNT network	Pre-stretched PDMS thin film	Dropping	10^3	$0 < \varepsilon < 2\%$	5% / 2300	[9]/2018
Porous carbon	PI	Direct laser writing	5000-10000	$\varepsilon < 0.1\%$	Not tested	[1]/ 2017
Cracked Au , Ag and Pt layered film;	PET	Thermal evaporation	1600	$\varepsilon=2\%$	2% / 5000	[10]/2017
Channel Crack-Designed Gold@PU Sponge	PU sponge	Ion sputtering	1	$\varepsilon<5\%$	45% /1000	[11]/2017
Graphite thin films with parallel microcracks	Ecoflex® elastomer film	Bar coating	<80	$0 < \varepsilon < 5\%$	Not tested	[12]/2016
Channel crack based gold film	PDMS	Electron beam evaporation	1000	$0.5\%<\varepsilon<0.7\%$	0.5% /1000	[13]/2016
			5000	$0.7\%<\varepsilon<1\%$		
Gold film	Microstruct-ured PDMS	Depositing	< 5	5%	Not tested	[14]/2015
Thickness-Gradient cnts Film	PDMS	Dropping	100	$0 < \varepsilon < 2\%$	2% / 100000	[15]/2015
Nano graphene film	PDMS	CVD and thansferring	600	$\varepsilon < 1\%$	0.3% /10000	[16]/2015
Monolayer Au nanoparticle	PET	Chemical synthesis	300	$\varepsilon < 0.3\%$	Not tested	[17]/2015
Ion-based Ag nano-ink	PDMS stamp	Spin-coating	0.06	$\varepsilon=5\%$	10% /1000	[18]/2014
Graphene rubber composites	Rubber band	Liquid exfoliation And infusion	20	$\varepsilon < 5\%$	75% /1000	[19]/2014
Cracked Pt layer	PUA	Sputtering	>2000	$0 < \varepsilon < 2\%$	2% /5000	[20]/2014

Cracked thin gold film	PU foam	Evaporation	<200	$0 < \varepsilon < 5\%$	20% /1000	[21]/2013
Graphene woven fabrics	Prestretched PDMS	CVD	10^0~10^3	$0 < \varepsilon < 5\%$	Not tested	[22]/2012
Micro channel liquid metal	Silicone rubber	Injecting	3	$\varepsilon < 5\%$	Not tested	[23]/2012
Graphene film	None substrate	Mechanically exploited	150	$0 < \varepsilon < 3\%$	Not tested	[24]/2011
Aligned CNT thin film	PDMS	CVD	60	$\varepsilon < 5\%$	150% /10000	[25]/2011
Cross-stacked super aligned CNT film	PDMS	Pouring	0.4	$\varepsilon < 5\%$	15% /200	[26]/2011
Zno/PS nanowire	PDMS	Electrospinning and hydrothermal reaction	116	$\varepsilon < 5\%$	4% /120	[27]/2011
BEDT-TTF composite bilayer film	PC	-	1800	$0 < \varepsilon < 0.5\%$	0.5% / > 270	[28]/2010

Reference

1. X. Duan, J. Luo, Y. Yao and T. Liu, *ACS Appl. Mater. Interfaces*, 2017, **9**, 43133-43142.
2. J. Luo, Y. Yao, X. Duan and T. Liu, *J. Mater. Chem. C*, 2018, **6**, 4727-2736.
3. S. Luo, P. T. Hoang and T. Liu, *Carbon*, 2016, **96**, 522-531.
4. Q. Li. Y. Gao, R. Wu, J. Sha, Y. Lu, and F. Xuan, *Adv. Funct. Mater*, 2018, 1806786.
5. B. Park, S. Lee, H. Choi, J. U. Kim, H. Hong, C. Jeong, D. Kang and T. I. Kim, *Nanoscale*, 2018, **10**, 4354-4360.
6. Z. Han, L. Liu, J. Zhang, Q. Han, K. Wang, H. Song, Z. Wang, Z. Jiao, S. Niu and L. Ren, *Nanoscale*, 2018, **10**, 15178-15186.
7. B. Zhang, J. Lei, D. Qi, Z. Liu, Y. Wang, G. Xiao, J. Wu, W. Zhang, F. Huo and X. Chen, *Adv. Funct. Mater*, 2018, **28**, 1801683.
8. Z. Ma, A. Wei, J. Ma, L. Shao, H. Jiang, D. Dong, Z. Ji, Q. Wang and S. Kang, *Nanoscale*, 2018, **10**, 7116-7126.
9. Y. Jiang, Z. Y. Liu, N. Matsuhisa, D. P. Qi, W. R. Leow, H. Yang, J. C. Yu, G. Chen, Y. Q. Liu, C. J. Wan, Z. J. Liu and X. D. Chen, *Adv. Mater*, 2018, **30**, 8.
10. T. Lee, Y. W. Choi, G. Lee, S. M. Kim, D. Kang and M. Choi, *Rsc. Adv*, 2017, **7**, 34810-34815.
11. Y. H. Wu, H. Z. Liu, S. Chen, X. C. Dong, P. P. Wang, S. Q. Liu, Y. Lin, Y. Wei and L. Liu, *ACS Appl. Mater. Interfaces*, 2017, **9**, 20098-20105.
12. M. Amjadi, M. Turan, C. P. Clementson and M. Sitti, *ACS Appl. Mater. Interfaces*, 2016, **8**, 5618-5626.
13. T. Yang, X. Li, X. Jiang, S. Lin, J. Lao, J. Shi, Z. Zhen, Z. Li and H. Zhu, *Mater. Horiz*, 2016, **3**, 248-255.
14. H. L. Filiatrault, R. S. Carmichael, R. A. Boutette and T. B. Carmichael, *ACS Appl. Mater. Interfaces*, 2015, **7**, 20745-20752.
15. Z. Liu, D. Qi, P. Guo, Y. Liu, B. Zhu, H. Yang, Y. Liu, B. Li, C. Zhang and J. Yu, *Adv. Mater*, 2015, **27**, 6230.
16. J. Zhao, G. Wang, R. Yang, X. Lu, M. Cheng, C. He, G. Xie, J. Meng, D. Shi and G. Zhang, *ACS nano*, 2015, **9**, 1622-1629.
17. L. Yi, W. Jiao, K. Wu, L. Qian, X. Yu, Q. Xia, K. Mao, S. Yuan, S. Wang and Y. Jiang, *Nano. Res*, 2015, **8**, 2978-2987.
18. J. Lee, S. Kim, J. Lee, D. Yang, B. C. Park, S. Ryu and I. Park, *Nanoscale*, 2014, **6**, 11932-11939.
19. U. K. Conor, S. Boland, C. Backes, A. O'Neill, J. McCauley, S. Duane, R. Shanker, Y. Liu, I. Jurewicz, A. B. Dalton and J. N. Coleman, *ACS nano*, 2014, **8**, 8819.
20. D. Kang, P. V. Pikhitsa, Y. W. Choi, C. Lee, S. S. Shin, L. Piao, B. Park, K.-Y. Suh, T. I. Kim and M. Choi, *Nature*, 2014, **516**, 222.
21. H. Vandeparre, Q. Liu, I. R. Minev, Z. Suo and S. P. Lacour, *Adv Mater*, 2013, **25**, 3117-3121.

22. X. Li, R. J. Zhang, W. J. Yu, K. L. Wang, J. Q. Wei, D. H. Wu, A. Y. Cao, Z. H. Li, Y. Cheng, Q. S. Zheng, R. S. Ruoff and H. W. Zhu, *Scientific Reports*, 2012, **2**, 6.
23. P. Yong-Lae, C. Bor-Rong and R. J. Wood, *IEEE Sens. J.*, 2012, **12**, 2711-2718.
24. M. Huang, T. A. Pascal, H. Kim, W. A. Goddard and J. R. Greer, *Nano Lett.*, 2011, **11**, 1241-1246.
25. T. Yamada, Y. Hayamizu, Y. Yamamoto, Y. Yomogida, A. Izadi-Najafabadi, D. N. Futaba and K. Hata, *Nat Nanotechnol*, 2011, **6**, 296-301.
26. K. Liu, Y. Sun, P. Liu, X. Lin, S. Fan and K. Jiang, *Advanced Functional Materials*, 2011, **21**, 2721-2728.
27. X. Xiao, L. Yuan, J. Zhong, T. Ding, Y. Liu, Z. Cai, Y. Rong, H. Han, J. Zhou and Z. L. Wang, *Adv Mater*, 2011, **23**, 5440-5444.
28. E. Laukhina, R. Pfattner, L. R. Ferreras, S. Galli, M. Mas-Torrent, N. Masciocchi, V. Laukhin, C. Rovira and J. Veciana, *Adv. Mater*, 2010, **22**, 977.